Monte Carlo Simulation of the Formation of Snowflakes

KEN-ICHI MARUYAMA*

Frontier Research Center for Global Change, Yokohama, Japan

YASUSHI FUJIYOSHI

Frontier Research Center for Global Change/Institute of Low Temperature Science, Hokkaido University, Sapporo, Japan

(Manuscript received 20 May 2003, in final form 1 September 2004)

ABSTRACT

A stochastic microphysical model of snow aggregation that combines a simple aggregation model with a Monte Carlo method was developed. Explicit treatment of the shape of individual snowflakes in the new model facilitates examination of the structure of snowflakes and the relationships between the parameters of the generated snowflakes, such as mass versus diameter, in addition to comparisons with observations. In this study, complexities in the shape of snowflakes are successfully simulated, and the understanding of the evolution of their size distribution is advanced. The mean diameter of snow particles evolves more rapidly in the aggregate model than in the sphere model. However, growth rates of the aggregates greatly depend on the collision section of particles in aggregation. The mean mass of snowflakes in the aggregate model grows more slowly than the mass in the sphere model when the sum of the particle cross section is used as the collision cross section. The mean mass grows more quickly when a circle is used whose radius is the sum of the radii of two particles. Sensitivity experiments showed that aggregation also depends on the mean and standard deviation of the initial distribution, and on the density of constituent particles.

1. Introduction

The most fascinating characteristic of snowflakes and snow crystals is their shape. However, the complexity of their shapes makes it difficult to uniquely determine their mass–size and terminal velocity–size relationships. In addition, it is difficult to define the size of a snowflake. Although new instruments can measure the shape of snowflakes, they cannot automatically measure the mass of individual snowflakes. Therefore, a numerical model that can simulate the 3D shape of snowflakes is important for interpreting and making use of these observed data.

Observational studies have examined the size–mass, size–fall velocity, and size–number of particles relationships for snowflakes (e.g., Hobbs et al. 1974; Rogers 1974; Fujiyoshi and Wakahama 1985; Mitchell et al. 1990; Ishizaka 1995; Kajikawa et al. 1996; Fujiyoshi and Muramoto 1996). In contrast to these detailed observational studies, snowflake shape has been treated rather simply in models, even in cloud-resolving and detailed microphysical models. Furthermore, changes in the shape of snowflakes have also been treated relatively simply; many models treat snowflakes as spheres or oblate spheroids.

Passarelli (1978a,b) suggested that one-to-one fall speed and diameter–mass relationships are inadequate for modeling snowflake aggregation. Subsequently, Passarelli and Srivastava (1979) presented a mathematical framework for modeling the aggregation process; this framework considered a spectrum of fall velocities and sizes for particles of a given mass. They introduced a modified kernel in the stochastic collection equation and showed that the growth rate critically depends on the width of the fall speed spectrum. However, it is difficult to extend their analytical model to make comparisons with observational studies. Moreover, Sasyo (1971) suggested that two collision types occur during snow formation: random and orderly. Subsequently, Sasyo and Matsuo (1980, 1985) determined a new kernel for a stochastic collection equation that considered the observed variation in fall velocity. The width of the fall velocity spectrum and the density of particles were fixed or assumed in the calculation, although they actually change with time. In other words, their models did not incorporate feedback between

* Current affiliation: National Research Institute for Earth Science and Disaster Prevention, Tsukuba, Japan.

Corresponding author address: Ken-ichi Maruyama, National Research Institute of Earth Science and Disaster Prevention, 3-1 Tennoudai Tsukuba Ibaragi, 305-0006, Japan.
E-mail: maruyama@bosai.go.jp

snowflake shape and the probability of snowflake collision. Therefore, we developed a model that takes into account changes in the 3D shape and density of snowflakes, as well as their spectra.

In general, there are two methods used for calculating the evolution of the size distribution arising from collision and coalescence. One method numerically solves the stochastic collection equation (SCE; e.g., Bott 1998; Berry and Reinhardt 1974). The second method uses a Monte Carlo method with the algorithm developed by Gillespie (1975). The former method has been used in various numerical models (e.g., Khain and Sednev 1995; Reisen et al. 1996). In the former model, it is very difficult, if not impossible, to include the effect of snowflakes' shape in the evolution of their size distribution. The Monte Carlo method was rigorously derived from "the fundamental premise of the stochastic model" (Gillespie 1975). It is so flexible that it can include the shape explicitly, as shown below, but it demands huge computational resources. Aggregation models using the Monte Carlo method have been developed and have mainly been applied to the study of dust and aerosol formation (e.g., Richardson 1995; Nakamura 1996). The Monte Carlo method has not been applied to snowflake formation prior to this study. The model in this study does not incorporate other important growth processes, such as vapor deposition and riming, because of limited computer resources.

This paper is organized as follows: a stochastic microphysical model for snowflake aggregation is developed by combining a simple aggregation model with the Monte Carlo method, which is introduced in section 2. Several sensitivity experiments that considered ideal cases were conducted to examine the effect of shape on the temporal evolution of the size distribution and the physical properties of the quantitatively generated snowflakes. Settings and results of the sensitivity experiments are presented in section 3. Explicit treatment of the shape of individual snowflakes in the new model allows an examination of the structure of snowflakes and of the relationships between various parameters for the generated snowflakes, such as mass versus diameter, as well as a comparison with observations. Model results are compared with previous observations in section 4. Sections 5 and 6 include a discussion and concluding remarks, respectively.

2. Methods

A simple aggregation model is combined with the Monte Carlo method to quantitatively evaluate the effect of shape on the formation of snowflakes. First, Gillespie's Monte Carlo method is briefly described. Then, modified algorithms are presented and some of the assumptions made in the present model are outlined.

a. The Monte Carlo method of Gillespie (1975)

The probability $C(i, j)d\tau$ is defined as the probability that a pair of particles (i, j) collides in the next time increment $d\tau$. If all $C(i, j)$ for any pair of particles (i, j) are given, the collision process can be calculated accurately using the Monte Carlo method of Gillespie (1975).

The probability $C(i, j)d\tau$ for the collision of particles in clouds is given by the equation

$$C(i, j)d\tau = \frac{K(i, j)}{V} d\tau, \tag{1}$$

where $K(i, j)$ is a coalescence kernel and V is the volume of space; $K(i, j)$ is the product of the difference in the horizontal and vertical velocities, the coalescence efficiency, and the cross sections of the particles.

If there are N particles in volume V at time t, then the infinitesimal time interval $t + \tau \sim t + \tau + d\tau$ by which the next collision will occur is determined by

$$\tau = \frac{-\ln r_1}{C_0}, \tag{2}$$

where r_1 is a uniform random variable that takes values from 0 to 1 and C_0 is defined as

$$C_0 = \sum_{i=2}^{N} \sum_{j=1}^{i-1} C(i, j). \tag{3}$$

Here, C_0 is the probability that any pair of particles will collide in the next infinitesimal time interval *dt;* and C_{ij}, the probability that the next collision at $t + \tau \sim t + \tau + d\tau$ occurs between a specified pair of particles, (i, j), is given by

$$C_{ij} = \frac{C(i, j)}{C_0}. \tag{4}$$

The calculation procedure is as follows:

1) Set time $t = 0$. Specify the initial masses $M_1, M_2, \ldots, M_N$ in volume V and a stopping time t_{stop}.
2) Evaluate C_0 and derive a random waiting time τ using Eq. (2). Replace t with $t + \tau$.
3) Specify the pair of particles (i, j) that will collide with probability C_0, defined in step 2.
4) Remove the pair of particles (i, j) and add a new particle with mass $M_i + M_j$ to the list of particles. Reduce the number of particles by 1.
5) Return to step 2, unless the simulation time t exceeds the stopping time $t_{\text{stop.}}$

b. Modified method

Gillespie's Monte Carlo method has been applied to studies of droplet growth (Valious and List 1984; Xia and Srivastava 2000). In this paper, the method is modified to consider the shape of generated particles.

Particles were assumed to be initially spherical, and density was used as a parameter, although the ice crys-

tals and snow particles that actually comprise a snowflake have complex shapes. The effect of this simplifying assumption on the calculation results will be discussed later. Several factors determine snowflake aggregation, such as the difference in the horizontal and vertical velocities, the coalescence efficiency E_{coal}, and the cross section of the snow particles. These are considered and the modified algorithm is described.

The velocity of snow particles also depends on environmental wind and turbulence. Although we can safely assume that the mean wind motion does not affect the collision process, fluctuations in wind velocity because of turbulence may enhance collisions. However, the effects of turbulence are not considered in this study because the effect of turbulent motion on snow particles is quite difficult to formulate. Instead, the probability of collision coalescence is considered as described below. As a result, the differences in the fall velocities equal the differences in the terminal fall velocities of the snow particles.

Terminal fall velocity in the present model is determined from the following equation, derived by Boehm (1989):

$$V = \frac{\text{Re}\eta}{2\rho_a}\left(\frac{\pi}{A}\right)^{1/2}, \tag{5}$$

$$\text{Re} = 8.5[(1 + 0.1519X^{1/2})^{1/2} - 1]^2,$$

$$X = \frac{8mg\rho_a}{\pi\eta^2}\left(\frac{A}{A_e}\right)^{1/4},$$

where Re, ρ_a, η, and g are the Reynolds number, ambient air density, viscosity, and gravitational constant, respectively. Also, A, A_e, and m are the cross section, effective cross section, and mass of snowflakes, respectively. The effective cross section, A_e, is defined in this paper as the area of the particle that is projected onto the plane, normal to the falling direction. The cross section, A, is defined as the area of the circle circumscribing A_e. The definition of A/A_e is similar to that for the case of snowflakes in Boehm (1989), that is,

$$\frac{A}{A_e} = \frac{4m}{\pi\rho R_{\text{max}}^3}, \tag{6}$$

where m, ρ, and R_{max} are the mass, density, and maximum distance between the center of gravity and the edge of a snowflake, respectively.

Past studies have suggested that the coalescence efficiency of ice/snow particles depends on temperature and the vapor pressure over ice (Hosler and Hallgren 1960). By contrast, Latham and Saunders (1970) found no such temperature dependence. Because the coalescence efficiency for snowflakes remains unknown, it is assumed to be 1. For the same reason, we do not consider snowflake breakup, which may be collision induced (Rogers and Yau 1989).

The cross section of a shape as complex as a snowflake is calculated as follows: it is not feasible to calculate the exact cross section of individual snowflakes in every time step, so two steps are taken. First, rough estimates of the cross section, Gillespie's Monte Carlo method, and random numbers are used to specify (i, j, τ_{close}) such that two particles (i, j) approach each other in the infinitesimal time interval $t + \tau_{\text{close}} \sim t + \tau_{\text{close}} + d\tau$. Then, the aggregation model is used to judge whether the two approaching particles will collide. The collision cross section of the two specified particles is roughly estimated to be equal to the area whose radius is the sum of the R_{max} for the two particles. This collision cross section is always larger than the exact cross section, so the probability derived using this cross section is not necessarily the probability of collision; it is the probability that the two specified particles will approach each other so closely that at least part of each particle passes through an area at the same time. In other words, it is the collision probability of an "envelope," which is a sphere of radius R_{max} that includes a snowflake.

Therefore, $C_{\text{close}}(i, j)d\tau$, the probability that two particles (i, j) will approach each other in the next infinitesimal time interval, $d\tau$, is given by

$$C_{\text{close}}(i, j) = \frac{E_{\text{coal}}\pi(R_{\text{max},i} + R_{\text{max},j})^2|\mathbf{V}_i - \mathbf{V}_j|}{V}, \tag{7}$$

where $\mathbf{V}_i$ and $\mathbf{V}_j$ are the fall velocity of two particles.

Then, C_{close} (i, j) and Gillespie's algorithm can be used to determine τ_{close}

$$\tau_{\text{close}} = \frac{-\ln r_1}{C_{\text{close},0}}, \tag{8}$$

where r_1 is a uniform random variable with values from 0 to 1 and $C_{\text{close},0}$is defined as

$$C_{\text{close},0} = \sum_{i=2}^{N}\sum_{j=1}^{i-1} C_{\text{close}}(i, j). \tag{9}$$

Here, $C_{\text{close},0}$ is the probability that any pair of particles will approach each other in the next infinitesimal time interval dt. Then, $C_{\text{close},ij}$, the probability that the next collision at $t + \tau_{\text{close}} \sim t + \tau_{\text{close}} + d\tau$ occurs between particles (i, j) is given by

$$C_{\text{close},ij} = \frac{C_{\text{close}}(i, j)}{C_{\text{close},0}}. \tag{10}$$

Whether these particles (i, j) really collide depends on the aggregation model.

Two aggregation models, A and B, are considered in this work. The collision cross section in model A is equal to the sum of the cross sections of two particles. In model B, the collision cross section is the circle whose radius is the sum of the radii of the two particles. If the particles rotate quickly enough, as compared to the relative velocity of the particles, or if they are perturbed by small-scale turbulence while passing each other, one particle may roll into the other. Therefore,

the cross section can be enhanced by the shape effect, which is the situation considered in model B. Muramoto et al. (1994) reported that rotational speed of a snowflake rapidly increases with decreasing cross-sectional area. Model B can be treated as the extreme case that maximizes the shape effect on the collision cross section in the aggregation. Whether two approaching particles really collide in model A is determined by the simple aggregation model described later.

If C_{aggr} is the probability that two specified particles collide in the aggregation model, the coalescence probability for the model A is

$$C(i, j) = C_{\text{close}}(i, j)C_{\text{aggr}}. \tag{11a}$$

In model B, particles always collide if they are within the area $\pi\ (R_{\text{max},A} + R_{\text{max},B})^2$. Therefore, the coalescence probability for model B is given by

$$C(i, j) = C_{\text{close}}(i, j). \tag{11b}$$

In both models, aggregate shape is generated in the same simple aggregation model.

The configuration of the simple aggregation model used in the present model is illustrated in Fig. 1. Two particles are arbitrarily specified as 1 and 2. The origin of the coordinate system is the center of gravity of particle 2. The center of gravity of particle 1 is placed randomly in the area $\pi\ (R_{\text{max},1} + R_{\text{max},2})^2$. Pruppacher and Klett (1997) noted the following on the topic of particle orientation: "For some hydrodynamic conditions, non-spherical particles may adopt a preferred orientation of fall in quiet air. However, under virtually all atmospheric conditions, there will be background turbulence as well, and this might be of sufficient intensity to significantly disrupt whatever orientation order the particles would otherwise possess". As a first step toward solving this difficult problem, the easiest assumption, namely random orientation, is adopted. Particles 1 and 2 are rotated once with uniform probability in all directions. When a collision occurs, the particles cease motion instantaneously and stick together at the contact point, based on the assumption that the coalescence efficiency is 1.

Because all of the particles comprising a snowflake are assumed to be rigid spheres, their shape is unaffected by a collision. The mutual geometric positions of the constituent particles are calculated and recorded. This yields complete information on the shape of the new aggregate.

The following is the modified process used for the calculation:

1) Set time $t = 0$. Specify a number N of initial masses and radii $(M_1, R_1), (M_2, R_2), \ldots, (M_N, R_N)$ in volume V, R_i is a maximum radius (R_{max}) of the particle i, which is the maximum distance from the center of gravity to the edge. Initially, all masses are spherical crystals. Specify a termination time t_{stop}.

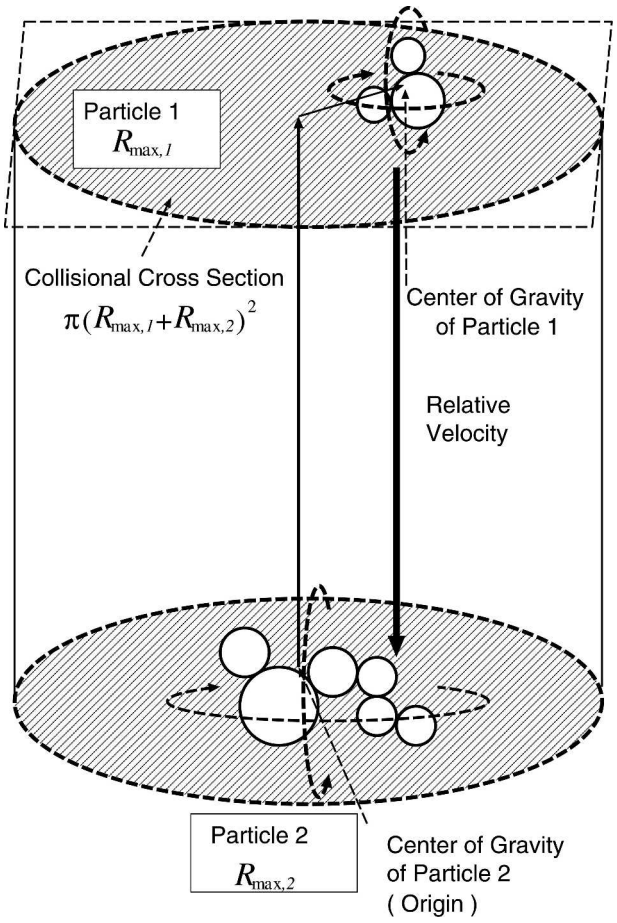

FIG. 1. Outline of the aggregation model.

2) Evaluate $C_{\text{close},0}$ using $R_1, R_2, \ldots, R_N$ and pick a random waiting time, τ_{close}, using Eq. (9). Replace t with $t + \tau_{\text{close}}$.
3) Specify the pair of particles (i, j) to collide with probability $C_{\text{close},0}$ from step 2. Note that model A and B differ on step 4.

4a) Check whether the particles collide using random numbers and the aggregation model. If they collide, determine the shape of the new aggregate. If not, return to step 2.

4b) Determine the shape of the new aggregate using the aggregation model. (Until a collision occurs, reselect random numbers.)

5) Remove (i, j) and add a new particle with mass $M_i + M_j$ to the list of particles. Calculate the maximum distance from the center of gravity to the edge of the new particle (R_{max}) and set this as the radius of the new particle. Reduce the number of particles, N, by 1.
6) Return to step 2, unless the simulation time exceeds the stopping time, t_{stop}.

Gillespie (1975) presented three algorithms for determining a triplet (i, j, τ). The partial conditioning

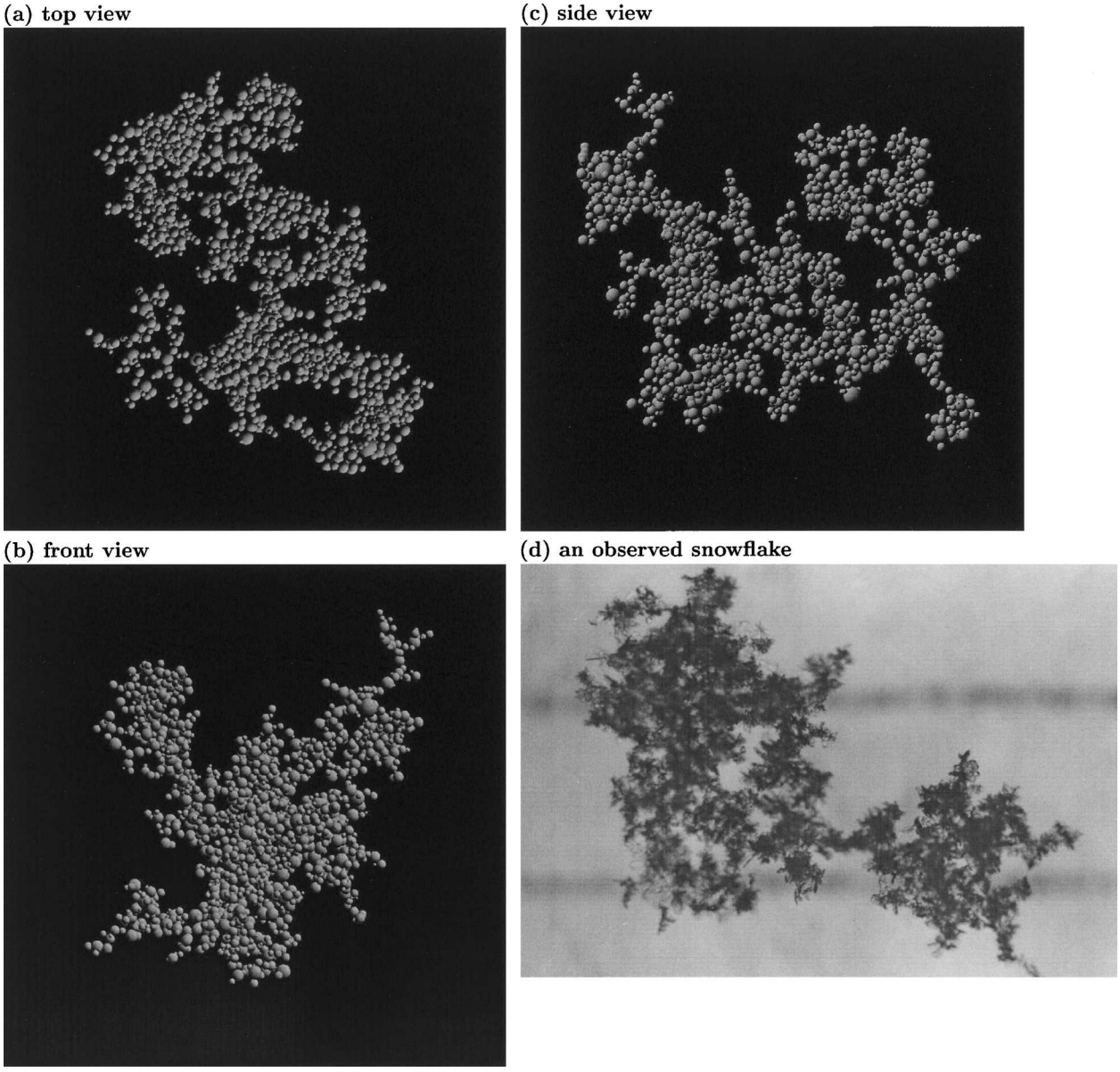

FIG. 2. Images in 3D of a generated snowflake consisting of 1760 particles: (a) top view and (b) front view. (c) A picture of an observed snowflake is also shown for comparison; the two faint lines behind the observed snowflake are separated by 5 mm.

method is used here because it was the most economic and effective in some test cases. The Monte Carlo solution method has some variation at the large end of the size distribution because large particles are scarce, as indicated by Valious and List (1984). In addition, fluctuations inherent in the Monte Carlo method necessitate several runs to derive a mean distribution suitable for comparison. Following Gillespie (1975), each simulation ran 10 times. The present algorithm has the advantage of retaining information about the shape of snowflakes. The computer code uses a linked list to record the position of constituent particles in an aggregate and to represent the shape, as undertaken by Richardson (1995). Figure 2 shows an example of a snowflake generated by the program that consists of 1760 constituent particles.

This method involves huge computational expense and cannot be coupled with 2D or 3D cloud-resolving models. However, this model can potentially improve the parameterization of aggregation because the characteristics of the generated snowflakes can be compared directly with observational data.

3. Comparisons of the model

To validate the model, results were compared to the analytical solution of the SCE (Golovin 1963) for the

TABLE 1. The initial conditions used in the numerical simulations. We assume that the mass volume density is 0.1 g m^{-3} and that the mean radius of the initial distribution is 1 mm.

	ρ: Density of constituent particles (g m^{-3})	Relative variance of initial distribution	Simulated volume (m^3)
CNTL	0.3	1.0	30
R1	0.1	0.5	50
R2	0.3	0.5	150
R3	0.5	0.5	250
V1	0.1	1.0	10
V2	0.1	0.5	10
V3	0.1	0.14	10

case $K = M_i + M_j$. Results showed good agreement with the analytical solution, except at the large end of the distribution.

Two kinds of model were run to show the effect of shape on growth rate clearly. One calculation used the model described above. A second calculation assumed that all snowflakes were spheres, that is, when two spherical snowflakes aggregate they form a larger sphere with a mass equal to the sum of the mass of the two particles. Hereafter, the former model is the aggregate model and the latter is the sphere model.

a. Initial size distribution of snow particles

A gamma distribution with a mass of 0.1 g m^{-3} and a mean size of 1 mm, which is based on a previous observational study (Fujiyoshi and Wakahama 1985), determines the initial size distribution of the snow particles making up snowflakes,

$$f(m) = \frac{N}{\overline{m}} \exp\left(-\frac{m}{\overline{m}}\right), \qquad (12)$$

$$N = \frac{Q}{\overline{m}},$$

where Q and N are the total ice water content and the total number of particles per unit volume, respectively, and m_f is the average mass. In the control (CNTL) case, we set the densities of the constituent particles at 0.3 g cm^{-3}.

Several sensitivity experiments were performed with different initial distributions and constituent particle densities. Table 1 summarizes the parameters used in these experiments. The following gamma distribution was used:

$$f(r) = \frac{N}{\overline{r}} \frac{(1+\nu)^{(1+\nu)}}{\Gamma(1+\nu)} s^{\nu} \exp[-(1+\nu)s], \qquad (13)$$

$$s = \frac{r}{\overline{r}}, \frac{4}{3}\pi\rho\overline{r}^3 = \frac{Q}{N},$$

where r_f is the average radius and ν is a parameter to specify the relative variance σ from the following equation (see e.g., Berry and Reinhardt 1974):

$$\sigma = \frac{\langle s^2\rangle - \langle s\rangle^2}{\langle s\rangle^2} = \frac{1}{1+\nu}. \qquad (14)$$

Because the rate of change of the size distribution depends on the mass volume density, the mass of snow particles in a volume of 1 m^3 was set to 0.1 g in all cases. The volume of the box was changed in these cases to keep the total number of particles roughly constant; otherwise, comparison would be difficult because of fluctuations that occur when using the Monte Carlo method.

b. Temporal evolution of the size distribution

Figure 3 shows the size distribution of the generated snowflakes after a 1.5-h simulation. The upper two and lower two panels show results from the aggregation (aggregate) models A and B, respectively. Results from the sphere model (sphere) are also shown. The values from the Monte Carlo model are the means of 10 runs. The SCE solution using the numerical method of Bott (1998) and the initial distribution (initial) are also shown in the figure. The ordinate denotes the mass density. The abscissas in the left and right panels are $R_{\max}$ and R_{melted}, respectively. The sphere model agrees well with the conventional solution of the SCE, which supports the validity of the numerics in the present model.

The growth of $R_{\max}$ and R_{melted} correspond to the growth of size and mass of a snowflake, respectively. Figure 3 indicates that particle size grows more quickly and mass grows more slowly in model A than in the sphere model. Both size and mass grow more quickly in model B than in the sphere model.

The mean of maximum diameter, $\overline{d_{\max}}$, and the diameter of mean mass, $D_{\overline{M}}$, which facilitate a quantitative discussion of the growth rate of snowflakes, are defined as

$$\overline{d_{\max}} = \frac{1}{N}\sum_{i=1}^{N} d_{\max,i}$$

$$D_{\overline{M}} = \left(\frac{6}{\pi\rho_w N}\sum_{i=1}^{N} M_i\right)^{1/3}, \qquad (15)$$

where $d_{\max,i}$ is the maximum distance between constituent particles, M_i is the mass of each particle, and ρ_w is the density of water ($\rho_w = 1.0$ g cm^{-3}). The distance between constituent particles 1 and 2 is defined as $|\mathbf{r}_1 - \mathbf{r}_2| + R_1 + R_2$, where $\mathbf{r}_j$, R_j are the position vector and the radius of constituent particle j respectively.

Figure 4 shows the temporal evolution of both $\overline{d_{\max}}$ and $D_{\overline{M}}$. Faster growth occurs in model B after 0.5 h (i.e., after more fluffy particles have formed). Interestingly, $\overline{d_{\max}}$ increases very quickly in the early growth stage (the first 20 min in model B). In the later growth stage (after 20 min in model B), $D_{\overline{M}}$ begins to increase rapidly. These stages correspond to the phases of random and orderly collisions (Sasyo 1971; Harimaya and Kawasato 2001; Kajikawa et al. 2002). As will be discussed in section 4c, the generated snowflakes grew in two dimensions in the early stage and in three dimen-

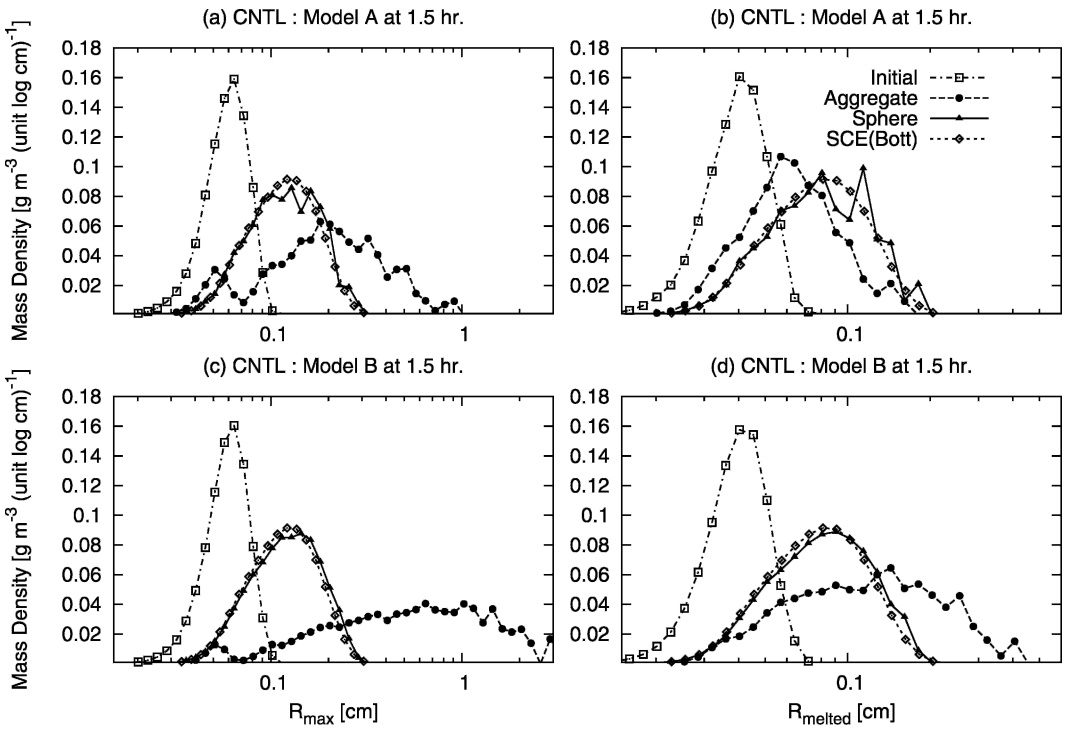

FIG. 3. Mass–size distribution of simulated snowflakes after 1.5 h by the aggregate models (a), (b) A and (c), (d) B. Mass density is shown as a function of (a), (c) R_{max} and (b), (d) R_{melted}. "Initial," "Aggregate," "Sphere," and "SCE (Bott)" denote the initial distribution of snowflakes, the results using the Monte Carlo model, the sphere model, and the numerical solution of the stochastic collection equation (SCE) of Bott, respectively.

sions in the later stage, as suggested by Kajikawa et al. (2002).

As noted in section 2, the coalescence kernel $K(i, j)$ depends mainly on the fall velocity and cross sections of the snowflakes. In section 5, we discuss which component is mainly responsible for the rapid growth of snowflakes in the aggregate model, and the dependency of the growth rate of snowflakes on the parameters of the initial distribution of the snow particles.

4. Comparison with observations

Mass and size, mass and cross section, and mass and terminal fall velocity are all related and, along with the structure of generated aggregates, are compared with observations in this section. It should be noted that the aggregation models A and B do differ. If the two models start with the same initial conditions, the maximum size and mass in model B grows more quickly than do those in model A. However, the aggregates in the two models have almost the same structure because they originate from the same simple aggregation model.

a. Mass–size and mass cross-section relationship

Figure 5a and Fig. 6 show the relationship between the maximum diameter and the mass of the generated snowflakes. Only particles that had more than 10 constituent particles have been plotted. Here, the maximum diameter, d_{max}, of a generated snowflake is defined as the maximum distance between any pair of constituent particles in the snowflake. Generally, $2R_{max} \geq d_{max}$ holds. The two-dimensional d_{max} in 2D is the average of three maximum distances, which are viewed from a set of three mutually orthogonal directions that are otherwise arbitrarily oriented. The d_{max} on 2D is plotted, for comparison, against the maximum distance on the picture and it is just a little smaller than d_{max}. Relationships derived from observations of unrimed and densely rimed dendritic crystals (Locatelli and Hobbs 1974; Fujiyoshi and Muramoto 1996) are shown for comparison. Note that Locatelli and Hobbs (1974) defined the aggregate diameter as the "diameter of the smallest circle into which the aggregate as photographed will fit without changing its density," while Fujiyoshi and Muramoto (1996) defined the diameter as the maximum distance measured from pictures that were taken from one side by a video camera. The points were fitted to the function $D = aM^b$ using the least squares method. The general trend in the relationship and the values of d_{max} and M for the generated snowflakes were similar to observations.

Figure 6a shows the effect of the density of the constituent snow particles on the relationship. When the mass is the same, d_{max} increases with decreasing density

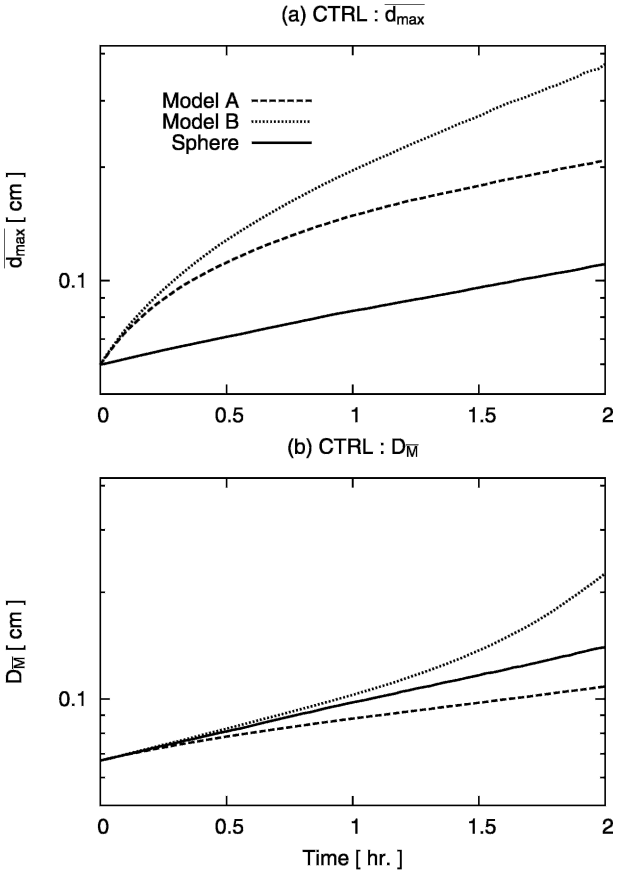

FIG. 4. Temporal change in (a) the mean of maximum diameter and (b) the melted diameter of mean mass ($D_{\overline{M}}$) for the aggregate and sphere cases.

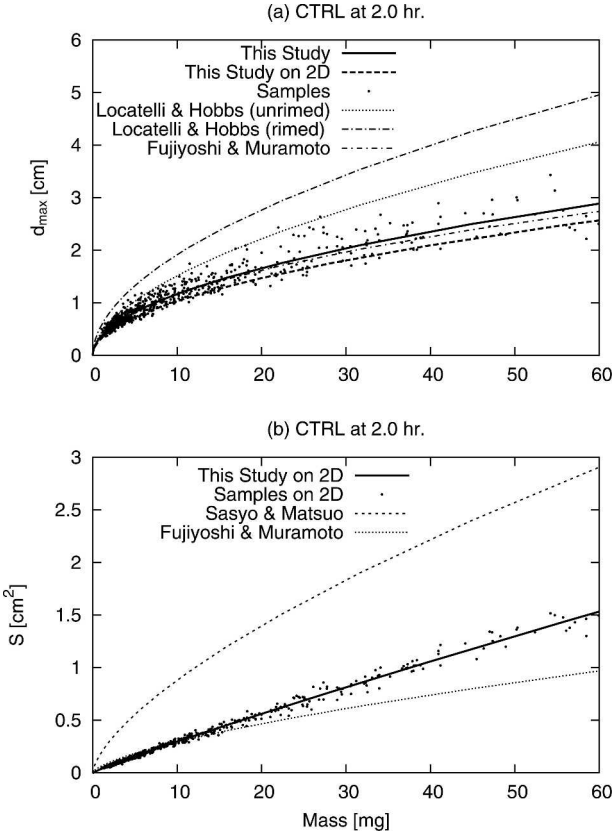

FIG. 5. Plot of (a) mass vs maximum diameter and (b) mass vs cross section for simulated snowflakes after hours of calculation for the control case with model B. Observational data are also plotted in the figure. (Unrimed and densely rimed aggregates in Locatelli and Hobbs 1974; Fujiyoshi and Muramoto 1996; Sasyo and Matsuo 1980).

of the constituent particles. The effect of relative variation, that is, the spectrum width of the initial size distribution, is shown in Fig. 6b. A smaller relative variation yields a larger $d_{\max}$. In other words, differences in the density and relative variations in the initial size distribution of the constituent snow particles can explain the discrepancy in the observed relationships.

Figure 5b shows the relationship between the cross section and the snowflake mass. Cross section is defined here as the average of three cross sections, which are viewed from a set of three mutually orthogonal directions that are otherwise arbitrarily oriented. The cross section is calculated as follows: 1) the maximum radius of the cross section, $RX_{\max}$, is calculated. 2) The aggregate is covered with a grid with a mesh size of $RX_{\max}/512$. 3) The cross section is calculated by counting the grid points that include part of the aggregates. The general trend in the relationship and the values of the cross section were also similar to observations.

b. The relationship between the diameter and terminal fall velocity

In the numerical experiments, terminal fall velocity was calculated using Eq. (5), derived by Boehm (1989). For this calculation, the cross section was calculated using Eq. (6) for an oblate spheroid snowflake. However, snowflakes generated in the model are not oblate spheroids. Therefore, the fall velocity of a snowflake computed using Eq. (6) might not agree with the observed velocity.

Calculated and observed fall velocities are shown in Fig. 7. The density of the constituent particles varied in the calculations from 0.1 to 0.5 g cm^{-3}. The fall velocities of the generated snowflakes showed a weaker size dependency than in observations. Indeed, the size–fall velocity relationship of the generated snowflakes was essentially invariable with time, and the relationship was consistent with the observed relationship only when the density of the constituent particles was 0.1 g cm^{-3}. As expected, snowflakes consisting of denser snow particles fall faster, but the calculated terminal velocity deviated from the actual value because snowflakes were approximated as oblate spheroids. Deviation is inevitable as long as this approximation is used. A more realistic representation of the constituent shape of snow particles, as columns or plates, would minimize the deviation. This improvement would probably be

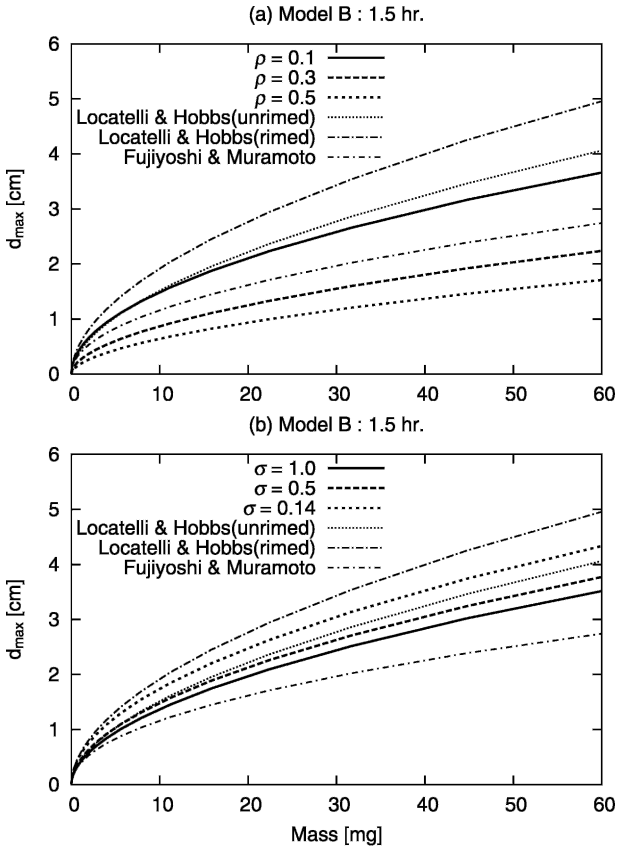

FIG. 6. Sensitivity tests on the plot of mass vs maximum diameter (the same as Fig. 5a). Only the lines fitted to $D = aM^b$ by using the least squares method are plotted (a) for three constituent particles (ρ = 0.1, 0.3, and 0.5 g cm^{-3}) and (b) for three relative variances (σ = 1.0, 0.5, and 0.14).

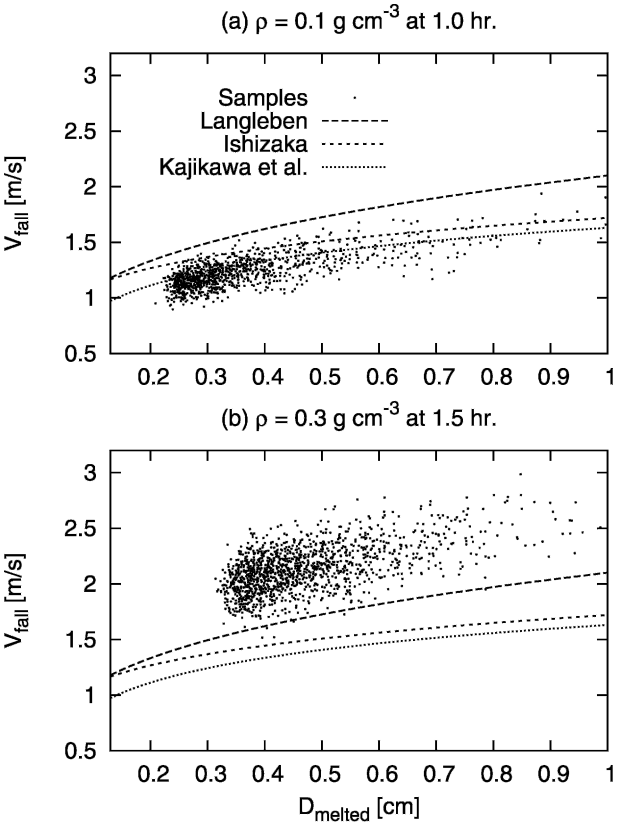

FIG. 7. The terminal fall velocity vs melted diameter of snowflakes after 2 h of calculation by model B. The density of the constituent particles is (a) 0.1 (R1 in Table 1) and (b) 0.3 g cm^{-3} (R2).

most effective in the early stages of aggregation, that is, at small size ranges. In addition, the cross section in Eq. (5) must be estimated directly with adequate precision using numerical methods. Observed fluctuation in the snowflake velocities should also be incorporated into the model.

c. Structure

As noted in section 3b, snowflakes' shape changes with time. The fractal dimension of the generated snowflakes was calculated because that dimension is a good index of shape complexity (e.g., Feder 1988).

Muramoto et al. (1993) analyzed digital images of individual falling snowflakes and quantified several physical parameters such as moment, concavity, compactness, and fractal dimension. Unlike other parameters, the fractal dimension is little affected by the camera direction or particle area. Table 2 lists the observed fractal dimensions for comparison. Muramoto et al. (1993) used the divider method to obtain fractal dimensions. The present study uses the box count method, which is as follows:

1) A grid is superimposed on the image; the initial grid is the maximum size of the image.
2) The number of grid squares that include the edge of a snowflake are counted.
3) The grid size is reduced.
4) Steps 1 to 3 are repeated to yield a relationship between grid size and the number of boxes.
5) The points are fitted to the equation $N = a\delta^{-b}$ using the least squares method, where δ, N, a, and b are the grid size, the number of grid squares that include an edge, and two constants, respectively.

Figure 8 shows how the above procedure is applied to an aggregate. Figure 8a shows the original image of the sample. Figures 8b–d show the image rim for three different mesh sizes, $RX_{max}/8$, $RX_{max}/32$, and $RX_{max}/512$,

TABLE 2. Observed fractal dimension of snowflakes [Table 2 in Muramoto et al. (1993)].

Direction	Snowflake A	Snowflake B	Snowflake C	Snowflake D
Top	1.12	1.14	1.15	1.13
Side	1.10	1.13	1.19	1.12

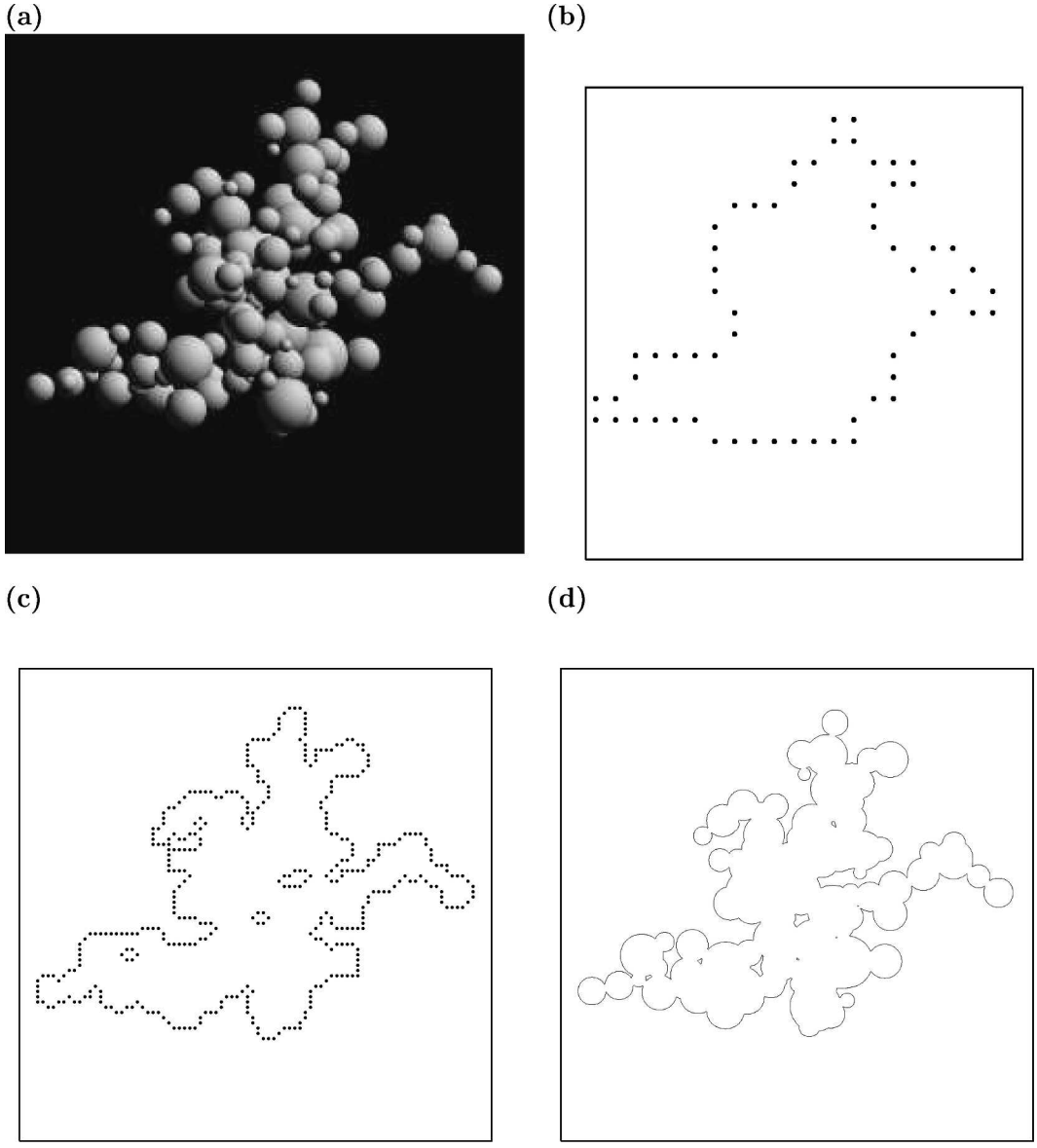

FIG. 8. (a) An aggregate consisting of 133 particles. (b) The rim of the aggregate represented with a grid of size $RX_{max}/8$; RX_{max} is the maximum radius of the image projected onto the YZ plane. (c) As in (b), but using $RX_{max}/32$. (d) As in (b), but using $RX_{max}/512$.

where RX_{max} is the maximum radius of the image projected onto the YZ plane. In Fig. 9a, the relationship between the number of grid boxes, including the rim, and the mesh size is shown for the aggregate in Fig. 8.

In the equation $N = a\delta^{-b}$, b is defined as the fractal dimension (Table 3). The observed fractal dimension in Table 2 compares favorably with results from the present model, despite differences in the method and the simplicity of the aggregation model used in this study. Figure 9b shows that the fractal dimension of an aggregate in our model increases with increasing numbers of constituent particles. The number of constituent particles increases with time in the model simulation; therefore, in Fig. 9b, this trend is consistent with observations reported in Kajikawa et al. (2002). They reported that snowflakes grew in two dimensions in the early stages and in three dimensions in later stages.

The change in density, with the radius of the sphere circumscribing a snowflake for the CNTL case (Figs. 10a,b), was calculated to determine whether snowflake density is homogeneous. The center of the sphere was located for this calculation at the center of gravity of the snowflake. The density profile is calculated as follows:

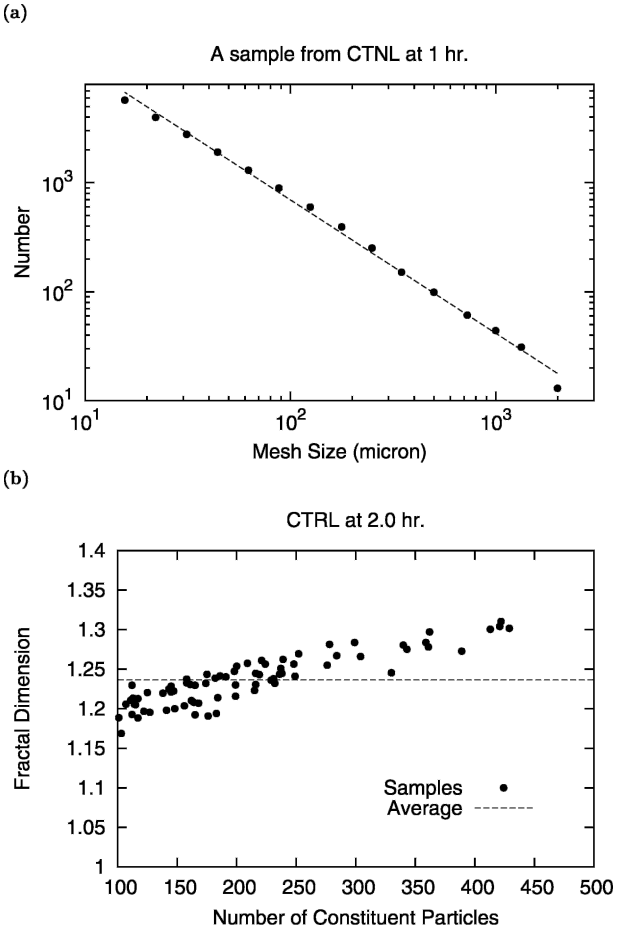

FIG. 9. (a) The relationship between the number of grid boxes including the rim and the mesh size is shown for the aggregate in Fig. 8. (b) The change in the fractal dimension with the number of constituent particles for the CNTL case after 2 h of calculation. Aggregates for which the melted diameter is between 3 and 5 mm and the number of constituent particles exceeds 100 are selected.

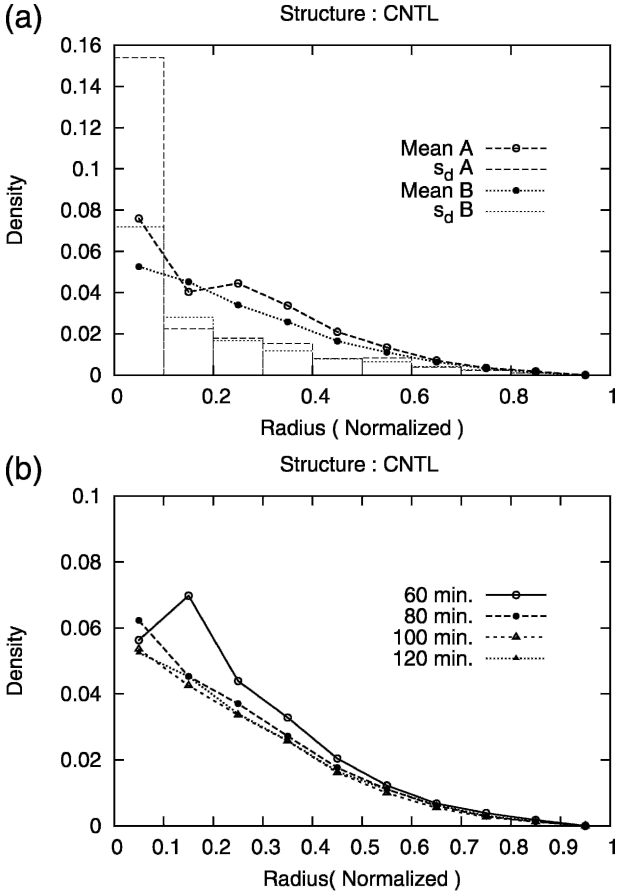

FIG. 10. (a) Change in the mean density of a particle (lines, mean) and its standard deviation (boxes, s_d) for the particles generated from two aggregation models, A and B, as a function of the radius of a sphere. The density and radius of the particles are normalized and averaged for all snowflakes with melted diameters from 3 to 5 mm. (b) Same as (a) for times from 60 to 120 min at 20-min intervals for the particles generated from model B.

1) The aggregate is segmented into a number of shells of constant thickness, from the center of gravity to the edge.
2) The density of each shell is calculated by dividing the sum of the particles that have a center of gravity in that shell by the shell volume. This method is not very accurate, especially when the number of constituent particles is small (the number 10 was used), but the structure of aggregates can be quickly approximated.
3) The particle radius was normalized and the average density profile was calculated for medium-sized snowflakes, ranging in size from 3 to 5 mm, to obtain a common structure among aggregates.

TABLE 3. Fractal dimension of simulated snowflakes for the CNTL case by model B. (a) Aggregates with diameters from 3 to 5 mm consisting of 50 ~ 100 particles. (b) The same as (a) for aggregates consisting of over 100 particles.

	Time	Number of aggregates	Fractal dimension			
			X	*Y*	*Z*	Mean
(a) 50 ~ 100	1.0 h	3	1.15	1.19	1.19	1.18
	1.5 h	3	1.18	1.19	1.15	1.17
	2.0 h	2	1.17	1.16	1.19	1.17
(b) 100~	1.0 h	16	1.20	1.20	1.20	1.20
	1.5 h	80	1.23	1.23	1.24	1.23
	2.0 h	75	1.24	1.23	1.24	1.24

Figure 10a shows that these snowflakes have similar structures, that is, the density decreases from the center to the edge. Figure 10b shows that the inner structure of the generated snowflakes does not change with time.

Sensitivity experiments were conducted by changing the parameters listed in Table 1 to study the dependency of structure on the parameters. A snowflake's mass becomes concentrated at its center as the density of the constituent particles increases (Fig. 11a). Figure

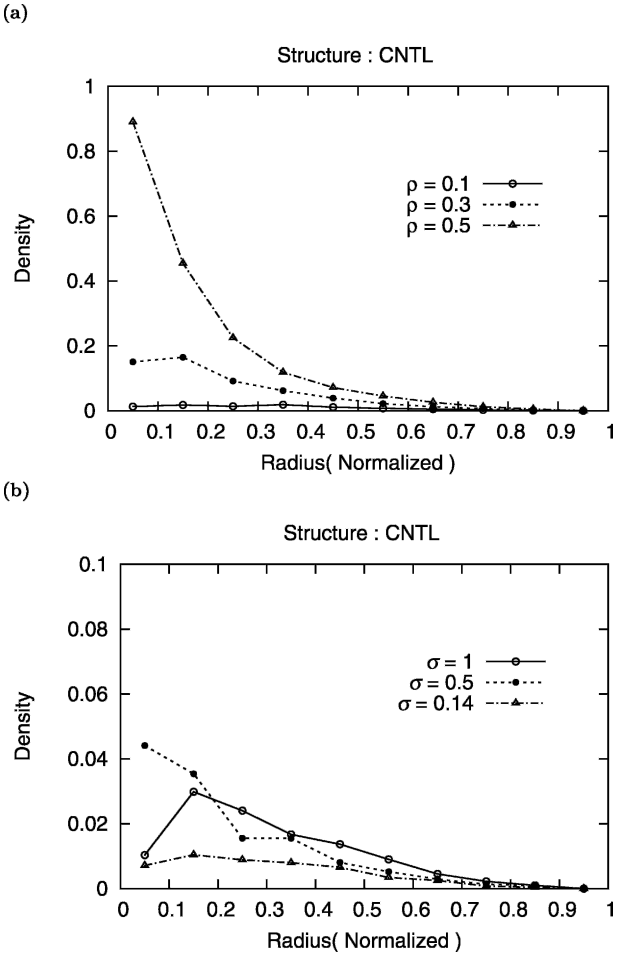

FIG. 11. As in Fig. 10 but for (a) three constituent particle densities (ρ = 0.1, 0.3, and 0.5 g cm^{-3}) and (b) three relative variances (σ = 1.0, 0.5, and 0.14) of the initial distribution for the particles generated from model B.

11b shows the effect of the relative variance of the initial size distribution. Snowflakes generated from a broader initial size distribution have a more homogeneous density with radius.

5. Discussion

a. Factors responsible for the growth in the aggregate model

Section 3b shows that in a sphere model, as compared to the aggregation model A, the mean radius of particles grows more quickly but the mean mass grows more slowly. The mean of both the radius and the mass grow more quickly in aggregation model B than in the sphere model. Coalescence depends mainly on differences in fall velocity and the collision cross section of snowflakes. A discussion of which component is mainly responsible for the growth of snowflakes in the aggregate models A and B follows.

Figure 12a shows the temporal evolution of the maximum cross section ($\equiv \pi R_{\max}^2$) and the average cross section in the aggregation (CNTL, ρ = 0.3 g cm^{-3}) and sphere models. Section 4a details how the cross section of each particle was calculated. Average cross sections were calculated only for generated particles that had more than 10 constituent particles. Because the calculation of actual snowflakes' cross sections is time-consuming, the cross sections were estimated at 30-min intervals. The actual cross section and the maximum cross section can be interpreted as the effective cross section in aggregation model A and B, respectively. The increase of the actual cross section in model A is a little smaller than the increase in the sphere model, but the increase of the maximum cross section in model B is much greater than the increase in the sphere model.

Two cross sections were defined in addition to the maximum and the average. The shape of a circumscribed snowflake must be adequately approximated if Boehm's equation is to be used to calculate the fall velocity. Effective cross sections I [$\equiv \pi R_{\max}^2$ $(3m/4\pi R_{\max}^3 \rho)^{2/3}$] and II [$\equiv \pi R_{\max}^2$ $(3m/\pi R_{\max}^3 \rho)^{2/3}$, the axis

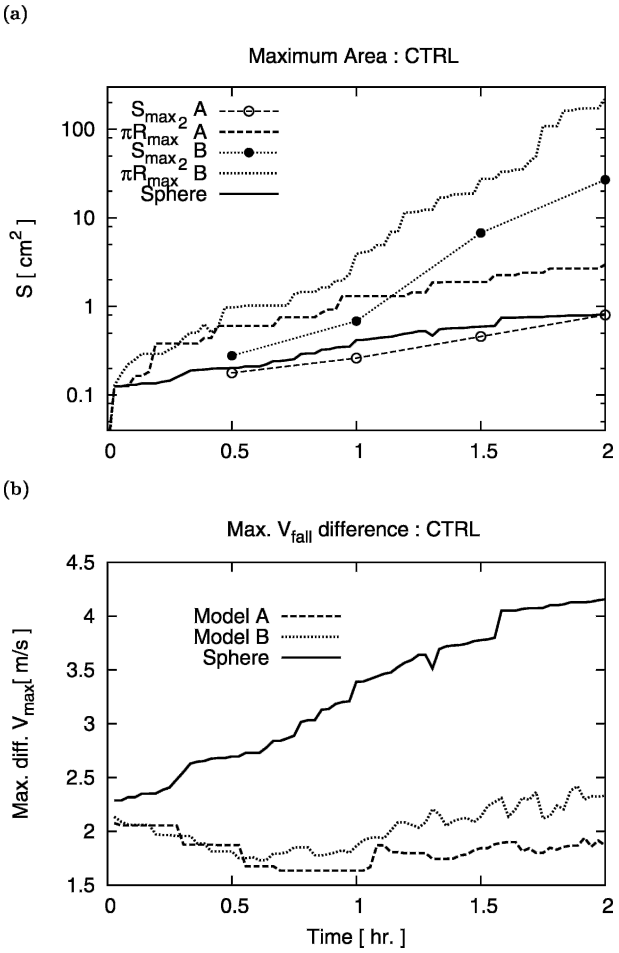

FIG. 12. Temporal change in (a) the maximum cross section and maximum $\pi R_{\max}^2$ and (b) the maximum difference in fall velocities between any pair of snowflakes for the aggregate and sphere cases.

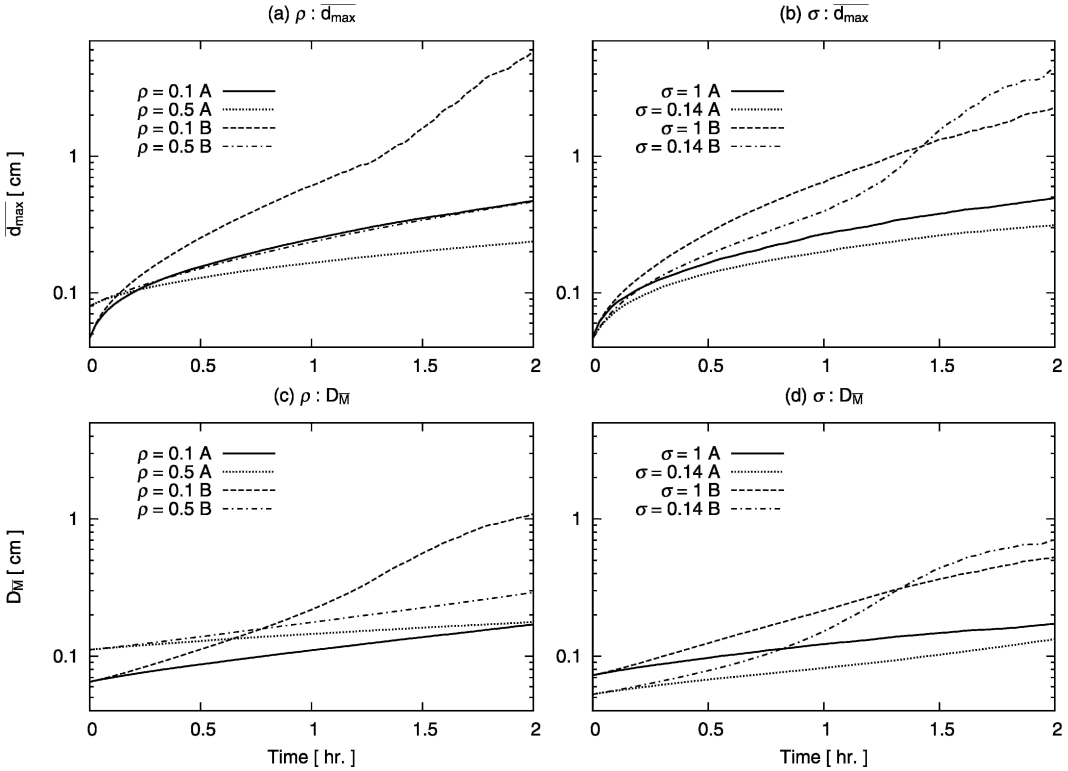

FIG. 13. Temporal change in (a), (b) the mean of maximum diameter ($\overline{d_{max}}$) and (c), (d) melted diameter of mean mass ($D_{\overline{M}}$) for constituent particles with (a), (c) two densities (ρ = 0.1 and 0.5 g cm^{-3}) and (b), (d) two relative variances (σ = 1 and 0.14) of the initial distribution.

ratio b/a = 0.25] were calculated for the CNTL case, assuming that the shape of a circumscribed snowflake was a sphere and oblate spheroid, respectively. The sphere approximation always underestimated the actual cross section of an aggregate; the oblate approximation yielded a better estimate of the actual snowflake cross section generated in the aggregation model.

Figure 12b shows the change in the maximum difference among snowflakes in terminal fall velocity with time. The difference increases with time in the sphere model. It does not increase with time in aggregate models A and B. The slow growth of mean mass in model A is driven mainly by a reduction of the relative velocity among particles, and fast growth in model B can be explained by the augmentation of the cross section. Differences in the cross section and the relative velocity were considered when reaching this conclusion. The large differences between the results of models A and B underscore the importance of the collision cross section in clearly estimating snowflake growth rates.

b. *Dependency of the growth rate on the initial distribution parameters*

The growth rate also depends on the parameters of the initial distribution listed in Table 1. Figure 13 shows the dependency of the temporal evolution of the mean maximum diameter and the melted diameter of mean mass on the density of the constituent particles and the relative variance of the initial distribution.

The effect of the density of the constituent particles (ρ = 0.1 and 0.5 g cm^{-3}) on the temporal evolution was investigated for a gamma distribution, with a mass volume density 0.1 g m^{-3}, a mean diameter of 1 mm and σ = 0.5. A decrease in the density of the constituent particles increased the growth rate of the size spectrum (Figs. 13a,c). The effect of the relative variance (σ = 1 and 0.14) on the temporal evolution was examined for the same initial distribution but with ρ = 0.1; the results are shown in Figs. 13b,d. Initially, the largest relative variance yielded the most rapid snowflake growth; however, in the later simulation stages, snowflakes grew more rapidly in model B with a small relative variance. Finally, the effect of the mean diameter of the initial distribution was examined by comparing cases with mean diameters of 1 and 2 mm; as expected, snowflakes grew faster in the latter case, consistent with observations (Rogers 1974; Hobbs et al. 1974; Kajikawa et al. 2002).

c. *Validity of the assumptions*

The validity of several assumptions is discussed in this section. One assumption is that a box model is used

for snow aggregation. Because the mass density per volume is constant at 0.1 g m^{-3}, the calculated volume could range from 1 to 250 m^3, that is, box size ranges from 1 to 10 m. Limited computer resources precluded the ability to follow the aggregational growth of all particles in a cloud or convective cell (less than 1 km^3). Collisions between particles were assumed to occur within a box; these particles did not interact with particles in other boxes. Bayewitz et al. (1974) suggested that in systems involving a small population, or in large systems that are poorly mixed, the full stochastic and kinetic models differ only at the large end of the size distribution. Gillespie (1975) also stated that this limitation might not be a serious problem because collision processes are local phenomena and that in reality, cloud particles do not interact with distant particles. However, their conclusions are supported only when particles are uniformly distributed in a box. Large snowflakes can fall out of the box, that is, boxes cannot be independent of each other in our model. Therefore, the present model implicitly assumes that snowflakes are homogeneously distributed within a cloud. If the difference in terminal fall velocity is assumed to be 0.5 m s^{-1} and the computation time is 1 h, the thickness of the homogeneous cloud should be 1.8 km. This limitation in the applicability is not serious for stratiform clouds, but it could be for convective clouds. If the mass volume density increases, the resulting growth rate increases because the increase in numerical density causes the growth rate of the size spectrum to increase more rapidly. The mass volume density was fixed at 0.1 g m^{-3}. If this mass density is increased, the thickness of homogeneous clouds is reduced, so that the limitation is not serious, even in a convective cloud.

A second assumption concerns the velocity of the aggregate. The simple aggregation model assumes random orientation and that the snowflakes generated in the model have complex shapes. On the other hand, the fall velocity was calculated using Eq. (6) for simplicity, and used as a mean fall velocity. Section 5b detailed how much the modeled fall velocity deviates from observation because of this assumption. The shape and orientation of snowflakes affect the fall velocity. Therefore, whenever modeled snowflakes change their shape and orientation, the collision probability should be recalculated. Steps to solve this problem could include 1) estimating the maximum fall velocity by minimizing the particle cross section by changing the orientation. 2) Estimating the maximum cross section of particles. 3) Estimating the probability of a close encounter using the maximum fall velocity and the maximum cross section. 4) Using the probability in step 3 to determine the time when the next close encounter will occur and specify the particles i, j to approach each other. 5) Judging whether the two particles collide using the adequate aggregation model. Two problems are thereby solved, namely the proper calculation of the cross section and the development of the most appropriate aggregation model.

A third assumption is the initial conditions. Unlimited computer resources would make it possible to perform numerous sensitivity experiments with different initial conditions. However, ice nucleation and vapor deposition must be considered as making the initial distribution more realistic. Xia and Srivastava (2000) developed a Monte Carlo method that included the condensation and the coalescence of water droplets. In principle, we could apply their method to a snow formation model. Unfortunately, only limited knowledge of the ice nucleation process exists. Therefore, more research is needed to improve the initial conditions of the model.

Finally, consider the assumption that a particle can approach another particle from any direction. This ignores the aerodynamics of snowflakes. Several studies have observed the coalescence and free-fall patterns of snowflakes (e.g., Higuchi 1960; Sasyo 1971; Kajikawa 1982, 1989, 1992). Kajikawa (1992) showed that, for dendritic snow crystals, the standard deviation of the horizontal velocity was considerably larger than that of the vertical velocity, and suggested that this property plays an important role in the random aggregation of platelike snow crystals of almost the same shape and size. In the present simulation, deviation in the velocity distribution of snowflakes arises only from differences in the fall velocity of snowflakes of different sizes and shapes. It is desirable to investigate the effect of observed deviations in the horizontal velocities of snowflakes.

Turbulence also affects the collection process. When the difference in the fall velocity is smaller than the fluctuations of the falling velocity of snowflakes "due to the shedding turbulent eddies in the wake" (Passarelli and Srivastava 1979), random collisions are mainly responsible for the growth of snowflakes. It would not be difficult in the present model to consider the spatial distribution of the collection probability mathematically and to change the probability with time. The combined effect of shape and turbulence should be assessed in the future, based on the results of sophisticated laboratory experiments and field observations.

6. Concluding remarks

A stochastic model for snow aggregation was developed by adding an aggregation model to the Monte Carlo method of Gillespie (1975). The model calculates both the temporal variation in the size spectrum and the complex shape of snowflakes. Simulated aggregates were surprisingly similar to natural ones (see Fig. 2). Sensitivity experiments were performed for some ideal cases. The conclusions are as follows:

1) The mean diameter of snow particles evolves more rapidly in the aggregate model than in the sphere

model. However, the growth rate of the aggregates greatly depends on the collision cross section of particles in aggregation. The mean mass of snowflakes in the aggregate model grows more slowly than in the sphere model when the sum of the cross sections of particles is used as the collision cross section. The mean mass grows more quickly in the aggregate model when a circle whose radius is the sum of the radii of the two particles is used.

2) Simulated size versus mass and mass versus cross-section relationships were compared with observations. If appropriate values for the parameters in the initial distribution are assigned, relationships consistent with observations can be reproduced.
3) The mass density of an individual snowflake decreases with the distance from its center of gravity. Sensitivity experiments indicate that the mass concentrates at the center of gravity when the density of the constituent particles is small and the relative variance of their size distribution is large.

In this model, we assumed that constituent particles are spherical with constant density. Future plans involve investigating the effect of ice crystal type on snow aggregation by introducing the shape of constituent ice particles, by representing columnar and plate shapes as a cluster of spheres. The box model will be extended to a 1D model to incorporate the effect of fallout of snowflakes. If vapor deposition and breakup are included in the model, model results could be compared to aircraft studies, during which clouds were observed several times with a spiral descent at the mean fall velocity of snowflakes to minimize the effects of the horizontal gradients and temporal changes (Houze et al. 1979; Lo and Passarelli 1982; Gordon and Marwitz 1986; Field 1999). A more complete model could be compared to other snow growth models (Lo and Passarelli 1982; Mitchell 1988, 1991), to further our understanding of snowflake formation.

We hope to develop a microphysical model that is consistent with snowflake shape observations. The present model could improve cloud microphysics parameterizations in a cloud-resolving model, although we still need to consider the effects of vapor deposition, riming, breakup, melting, and breakup during melting, and also make numerous comparisons with observations.

Acknowledgments. We are grateful to Dr. R. Nakamura (JAXA, Japan) for valuable discussion about Monte Carlo simulation and providing the program for aggregates. We also appreciate Dr. A. Bott (Bonn University, Germany) for providing his FORTRAN program to solve the stochastic collection equation. This work had been mainly done when first author worked at Frontier Research Center for Global Change, Japan, and was completed under the auspice of the National Research Institute for Earth Science and Disaster Prevention (NIED), Japan.

REFERENCES

Bayewitz, M. H., J. Yerushalmi, S. Katz, and R. Shinnar, 1974: The extent of correlations in a stochastic coalescence process. *J. Atmos. Sci.,* **31,** 1604–1614.

Berry, E. X., and R. L. Reinhardt, 1974: An analysis of cloud drop growth by collection. Part I: Double distributions. *J. Atmos. Sci.,* **31,** 1814–1824.

Boehm, J. P., 1989: A general equation for the terminal fall speed of solid hydrometeors. *J. Atmos. Sci.,* **46,** 2419–2427.

Bott, A., 1998: A flux method for the numerical solution of the stochastic collection equation. *J. Atmos. Sci.,* **55,** 2284–2293.

Feder, J., 1988: *Fractals*. Plenum, 310 pp.

Field, P. R., 1999: Aircraft observations of ice crystal evolution in an altostratus cloud. *J. Atmos. Sci.,* **56,** 1925–1941.

Fujiyoshi, Y., and G. Wakahama, 1985: On snow particles comprising an aggregate. *J. Atmos. Sci.,* **42,** 1667–1674.

——, and K. Muramoto, 1996: The effect of breakup of melting snowflakes on the resulting size distribution of raindrops. *J. Meteor. Soc. Japan,* **74,** 343–353.

Gillespie, D. T., 1975: An exact method for numerically simulating the stochastic coalescence process in a cloud. *J. Atmos. Sci.,* **32,** 1977–1989.

Golovin, A. M., 1963: The solution of the coagulation equation for cloud droplets in a rising air current. *Izv. Geophys. Ser.,* **5,** 482–487.

Gordon, G. L., and J. D. Marwitz, 1986: Hydrometeor evolution in rainbands over the California Valley. *J. Atmos. Sci.,* **43,** 1087–1101.

Harimaya, T., and Y. Kawasato, 2001: Snowflake formation and its regional characteristics. *J. Faculty Sci., Hokkaido Univ. Ser. VII Geophys.,* **11**, 793–809.

Higuchi, K., 1960: On the coalescence between plane snow crystals. *J. Meteor.,* **17,** 239–243.

Hobbs, P. V., S. Chang, and J. D. Locatelli, 1974: The dimensions and aggregation of ice crystals in natural clouds. *J. Geophys. Res.,* **79,** 2199–2206.

Hosler, C. L., and R. E. Hallgren, 1960: The aggregation of small ice crystals. *Discuss. Faraday Soc.,* **30,** 200–207.

Houze, R. A., Jr., P. V. Hobbs, P. H. Herzegh, and D. B. Parsons, 1979: Size distributions of precipitation particles in frontal clouds. *J. Atmos. Sci.,* **36,** 156–162.

Ishizaka, M., 1995: Measurement of falling velocity of rimed snowflakes (in Japanese). *Seppyo,* **57,** 229–239.

Kajikawa, M., 1982: Observation of the falling motion of early snow flakes. Part I: Relationship between the free-fall pattern and the number and shape of component snow crystals. *J. Meteor. Soc. Japan,* **60,** 797–803.

——, 1989: Observation of the falling motion of early snow flakes. Part II: On the variation of falling velocity. *J. Meteor. Soc. Japan,* **67,** 731–738.

——, 1992: Observations of the falling motion of plate-like snow crystals. Part I: The free-fall patterns and velocity variations of unrimed crystals. *J. Meteor. Soc. Japan,* **70,** 1–9.

——, S. Taniguchi, and S. Ito, 1996: Relationship between the fall velocity of snowflakes and the shape of their component crystals (in Japanese). *Seppyo,* **58,** 455–462.

——, E. Narita, K. Ichinoseki, S. Kudo, and R. Sasaki, 2002: Observation of composition factors of snowflakes (in Japanese). *Seppyo,* **64,** 69–76.

Khain, A. P., and L. L. Sednev, 1995: Simulation of hydrometeor size spectra evolution by water-water, ice-water and ice-ice interactions. *Atmos. Res.,* **36,** 107–138.

Latham, J., and C. P. R. Saunders, 1970: Experimental measurements of the collection efficiencies of ice crystals in electric fields. *Quart. J. Roy. Meteor. Soc.,* **96,** 257–265.

Lo, K. K., and R. E. Passarelli Jr., 1982: The growth of snow in

winter storms: An airborne observational study. *J. Atmos. Sci.,* **39,** 697–706.
Locatelli, J. D., and P. V. Hobbs, 1974: Fall speeds and mass of solid precipitation particles. *J. Geophys. Res.,* **79,** 2185–2197.
Mitchell, D. L., 1988: Evolution of snow-size spectra in cyclonic storms. Part I: Snow growth by vapor deposition and aggregation. *J. Atmos. Sci.,* **45,** 3431–3451.
——, 1991: Evolution of snow-size spectra in cyclonic storms. Part II: Deviations from the exponential form. *J. Atmos. Sci.,* **48,** 1885–1898.
——, R. Zhang, and R. L. Pitter, 1990: Mass-dimensional relationships for ice particles and the influence of riming on snowflake rates. *J. Appl. Meteor.,* **29,** 153–163.
Muramoto, K., K. Matsuura, and T. Shiina, 1993: Analysis of snowflake shape by a region and contour approach. *Trans. Inst. Electron. Inf. Commun. Eng., Sect. D* (Japanese edition), **J76-D-II**, 949–958.
——, S. Takagi, T. Shiina, and H. Matsuura 1994: Analysis of fall patterns of snowflakes. *Trans. Inst. Electron. Inf. Commun. Eng., Sect. D* (Japanese edition), **J77-D-II**, 1778–1787.
Nakamura, R., 1996: Fractal dust growth in the protoplanetary disk. Ph.D. thesis, Kobe University, 61 pp.
Passarelli, R. E., Jr., 1978a: An approximate analytical model of the vapor deposition and aggregation growth of snowflakes. *J. Atmos. Sci.,* **35,** 118–124.
——, 1978b: Theoretical and observational study of snow-size spectra and snowflake aggregation efficiencies. *J. Atmos. Sci.,* **35,** 882–889.
——, and R. C. Srivastava, 1979: A new aspect of snowflake aggregation theory. *J. Atmos. Sci.,* **36,** 484–493.
Pruppacher, H. R., and J. D. Klett, 1997: *Microphysics of Clouds and Precipitation*. Kluwer Academic, 954 pp.
Reisin, T., Z. Levin, and S. Tzivion, 1996: Rain production in convective clouds as simulated in an axisymmetric model with detailed microphysics. Part I: Description of the model. *J. Atmos. Sci.,* **53,** 497–519.
Richardson, D. C., 1995: A self-consistent numerical treatment of fractal aggregate dynamics. *Icarus,* **115,** 320–335.
Rogers, D. C., 1974: The aggregation of natural ice crystals. Research Rep. AR110, Dept. of Atmospheric Resources, University of Wyoming, 41 pp.
Rogers, R. R., and M. K. Yau, 1989: *A Short Course in Cloud Physics*. Butterworth Heinemann, 290 pp.
Sasyo, Y., 1971: Study of the formation of precipitation by the aggregation of snow particles and the accretion of cloud droplets on snowflakes. *Pap. Meteor. Geophys.,* **22,** 69–142.
——, and T. Matsuo, 1980: On the statistical investigation of fall velocity of snowflakes. *Pap. Meteor. Geophys.,* **31,** 61–79.
——, and ——, 1985: Effects of the variations of falling velocities of snowflakes on their aggregation. *J. Meteor. Soc. Japan,* **63,** 249–261.
Valious, I. A., and E. J. List, 1984: A numerical evaluation of the stochastic completeness of the kinetic coagulation equation. *J. Atmos. Sci.,* **41**, 2516–2529.
Xia, Q., and R. Srivastava, 2000: Monte Carlo simulation of cloud drop growth by condensation and coalescence. *Proc. 13th Int. Conf. on Clouds and Precipitation,* Reno, NV, International Association of Meteorology and Atmospheric Sciences, 169–172.